

Substrate-integrated hollow waveguides:

A new level of integration in mid-infrared gas sensing

Supporting Information

*Andreas Wilk¹, J. Chance Carter², Michael Chrisp², Anastacia M. Manuel², Paul Mirkarimi², Jennifer B. Alameda², Boris Mizaikoff^d**

¹Institute of Analytical and Bioanalytical Chemistry (IABC), University of Ulm,
Albert-Einstein-Allee 11, 89081 Ulm, Germany

²Lawrence Livermore National Laboratory (LLNL),
7000 East Avenue, Livermore CA 94550, USA

*Email: boris.mizaikoff@uni-ulm.de

ABSTRACT OF SUPPORT INFORMATION (SI). The SI contains a scheme of a four-piece iHWG prototype with yin-yang geometry, and depicts its assembly concept. Moreover, an AFM spectrum of a hand-polished surface, and a scheme explaining the radiation propagation within a meandered waveguide is shown. A spectrum of acetic acid is enclosed, followed by an extended list of parameters used for data acquisition. Spectra of various pure analytes diluted to 5000 ppm_v each are provided, and a trace level spectrum of one of those analytes (butane at 20 ppm_v). All spectra were obtained with the iHWG prototype discussed in the main article. Finally, the detection limit of butane is estimated.

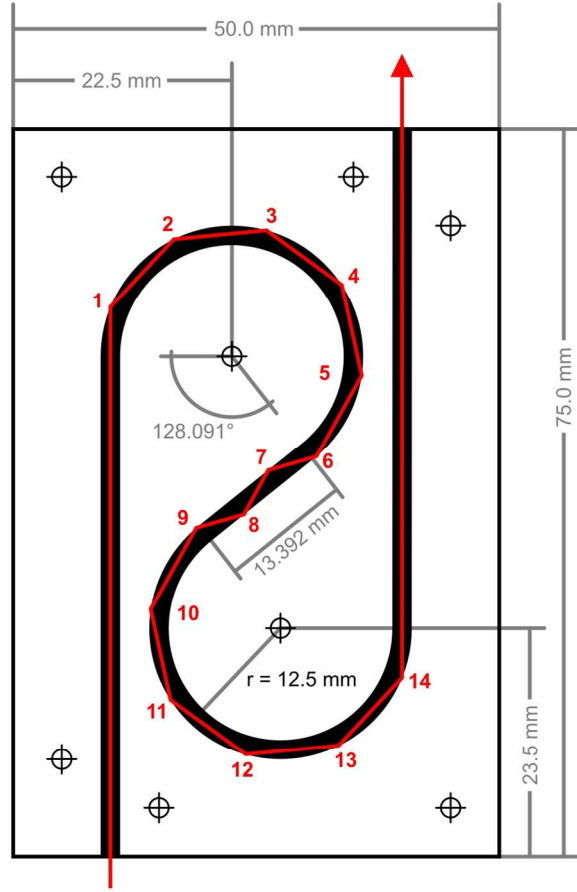


Figure S-1. Scheme of the prototype iHWG with substrate dimensions, channel geometry, and modeled propagation path of the center ray (numbers of reflections in red).

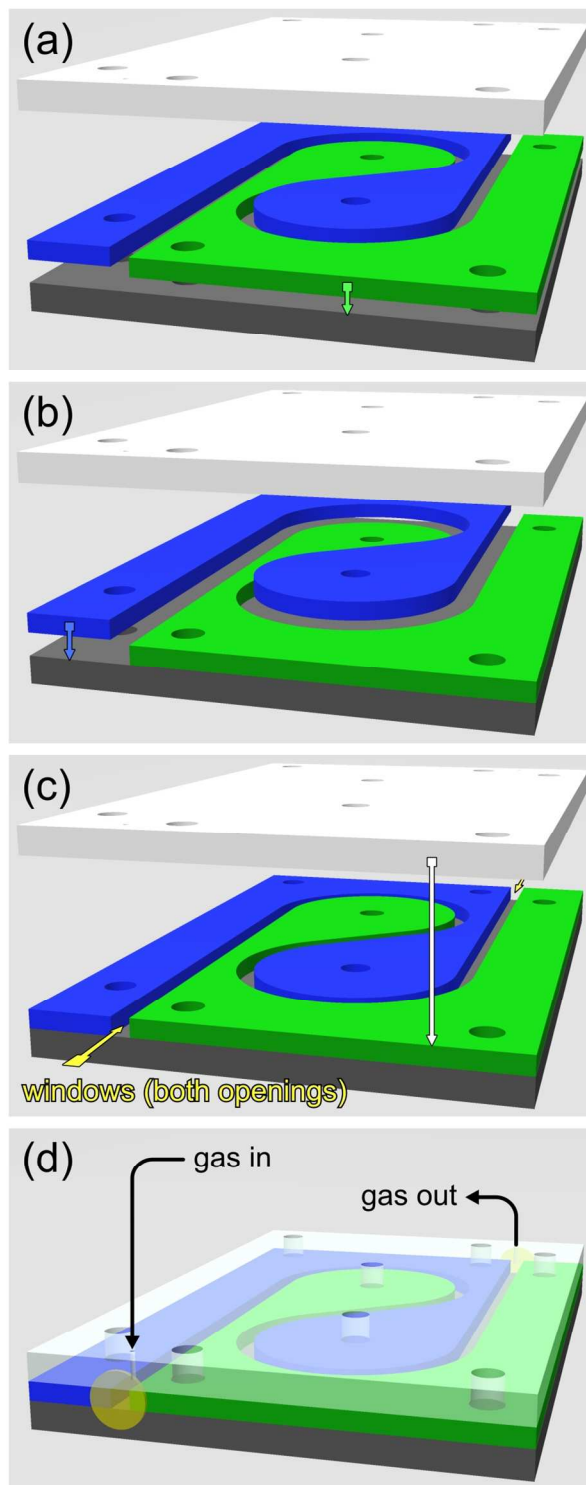


Figure S-2. (a-d) iHWG stacked assembly concept showing the top and base plates with internal waveguide sections (blue and green).

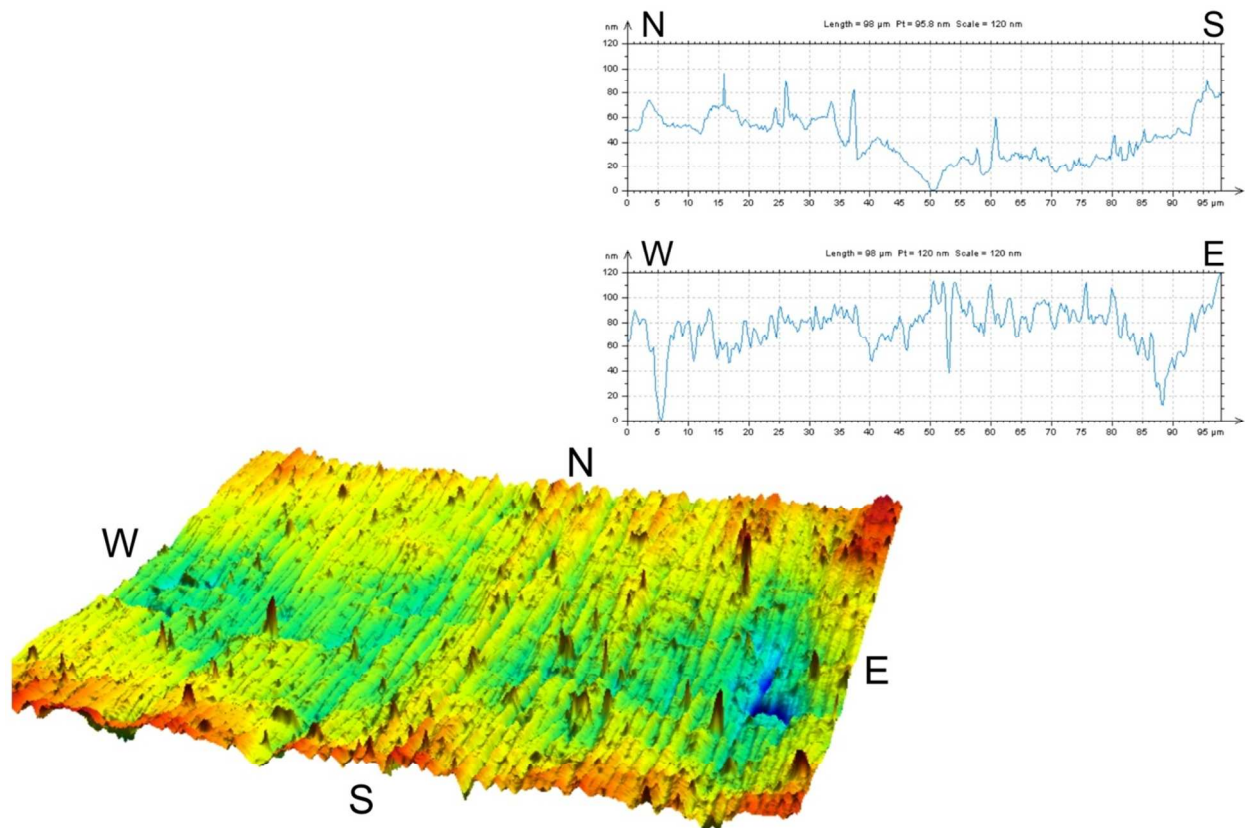


Figure S-3. Typical AFM image of a hand-polished surface element, including north/south and west/east cross sectional profiles. The root-mean-squared (RMS) surface roughness of this 98x98 μm area is 33 nm. It should be noted that the RMS value considers both roughness *and* surface flatness (i.e., waviness).

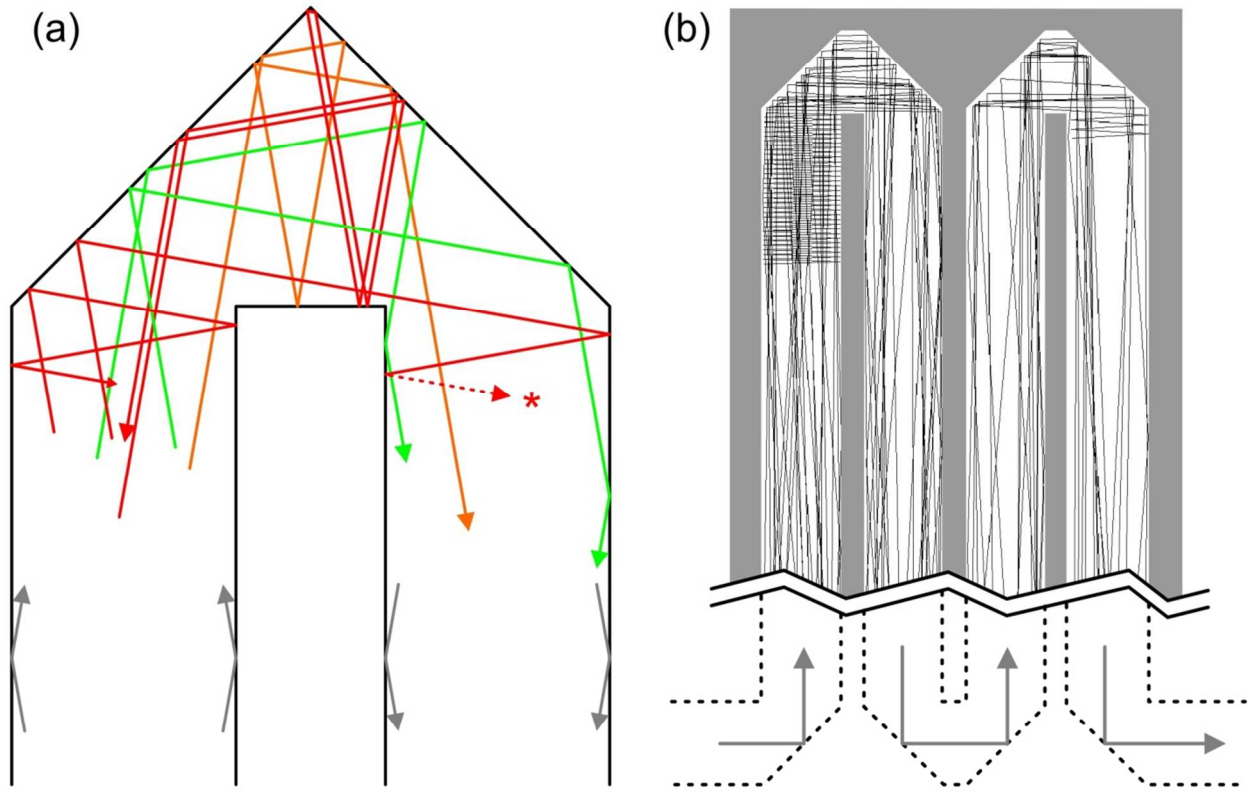


Figure S-4. (a) Schematic of 6 sample rays emerging from a non-collimated light source (10° beam divergence, which is approximately corresponding to the coupling conditions of an OAPM with 2" focal length and 2" effective focal length) propagating through a meandered (serpentine) waveguide channel with intact apex. Green: rays are propagated as desired, i.e. "around the corner"; orange: ray is suffering from multiple reflections, yet, finally successfully propagated; red: rays are either reflected back to the source, or (*) propagated such that their mean free OPL is significantly decreased. Both situations will cause a decrease in radiation throughput (i.e., geometric loss), as those rays will not reach the detector. (b) Semi-schematic ray tracing of 60 MIR test rays through a gold-coated meandered waveguide channel with flattened apex. Here, the radiation coupled into the device is almost collimated (1° cone angle). As a consequence, the serpentine structure is quite effective, and geometric losses are significantly reduced. Yet, a single back reflection remains evident in the left meander arm, and one reflection with a shorter mean free OPL is apparent in the right meander arm. Both rays add to the overall attenuation, as they are absorbed rather quickly. Spectrally resolved ray tracing was executed using SPRAY (W. Theiss Hard- and Software, Aachen, Germany).

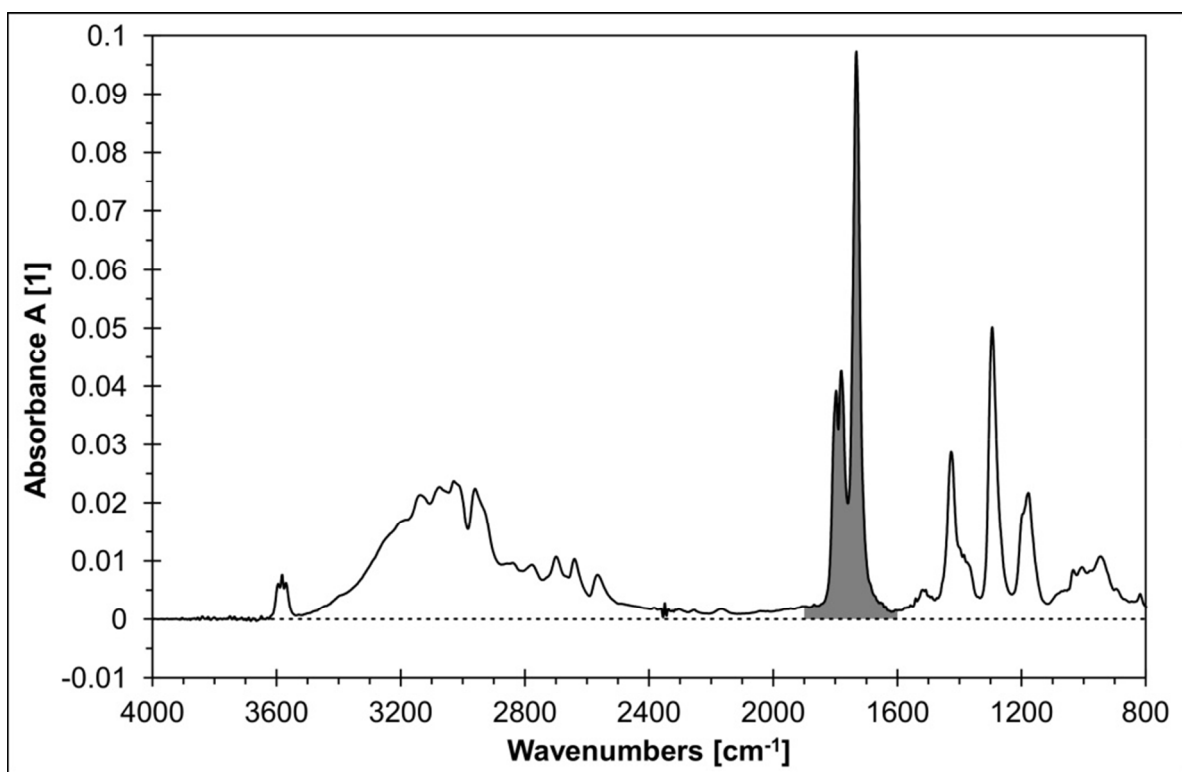


Figure S-5. Spectrum of acetic acid; iHWG. Datapoint: 1200s (compare Fig. 3).
Shaded: Integrated peak area (1600-1900 cm⁻¹).

Data acquisition parameter	Setting
Spectral resolution [cm^{-1}]	2
Sample scan time [scans]	100
Background scan time [scans]	100
Save data from [cm^{-1}]	4000
Save data to [cm^{-1}]	650
Aperture [mm]	3
Scanner velocity [kHz]	40
Preamp gain	Reference
Sample signal gain	x1
Background signal gain	x1
Wanted high frequency limit [cm^{-1}]	8000
Wanted low frequency limit [cm^{-1}]	0
High pass filter	Open
Low pass filter	Open
Acquisition mode	Double-sided, forward-backward
Correlation mode	Off
Phase resolution	8
Phase correction mode	Mertz
Apodization function	Blackman-Harris 3-term
Zerofilling factor	4

Table S-1. Fundamental spectra acquisition parameters (Bruker OPUS 6.5 software).

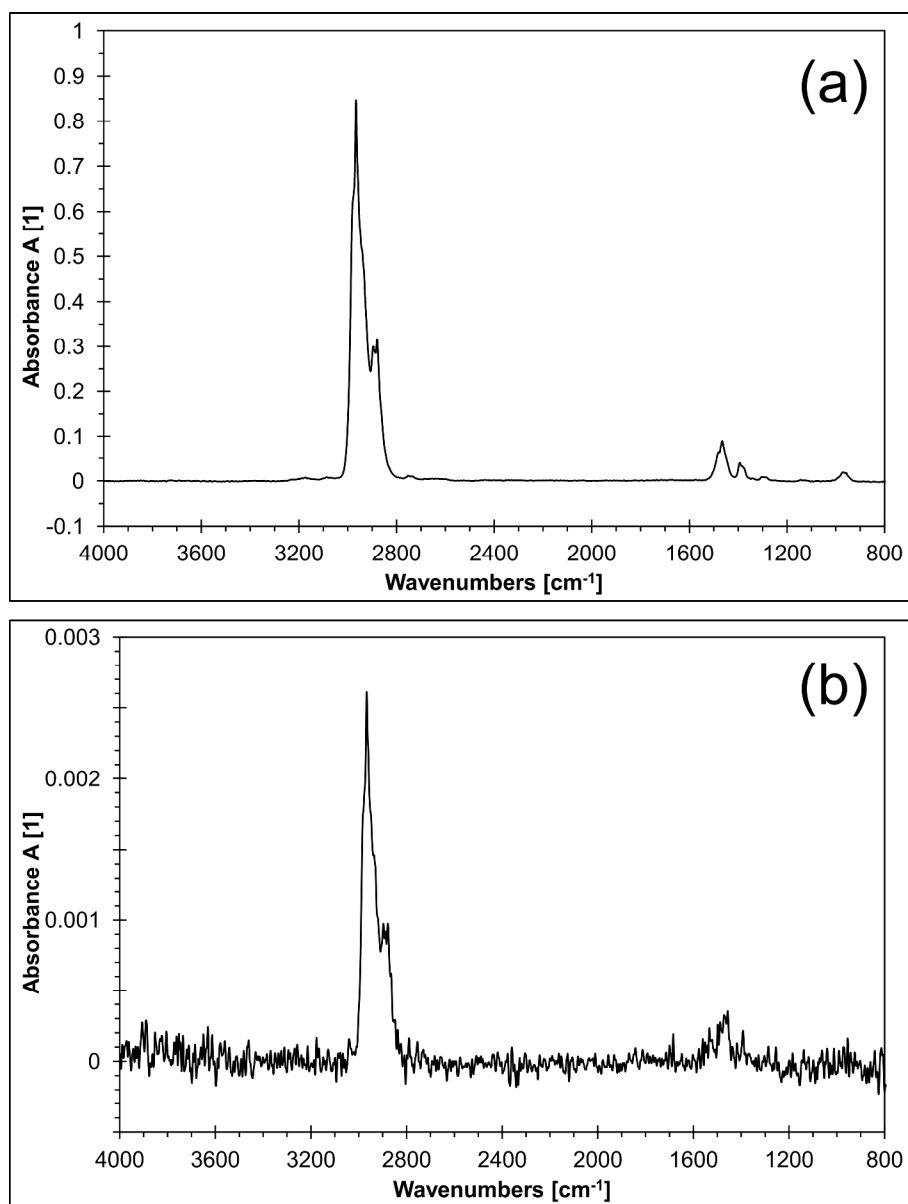


Figure S-6. (a) MIR absorption spectrum of butane diluted in N₂ to 5000 ppm_v obtained with the iHWG MIR sensor; 100 averaged scans. (b) MIR absorption spectrum of butane diluted in N₂ to 20 ppm_v obtained with the iHWG MIR sensor; 1000 averaged scans.

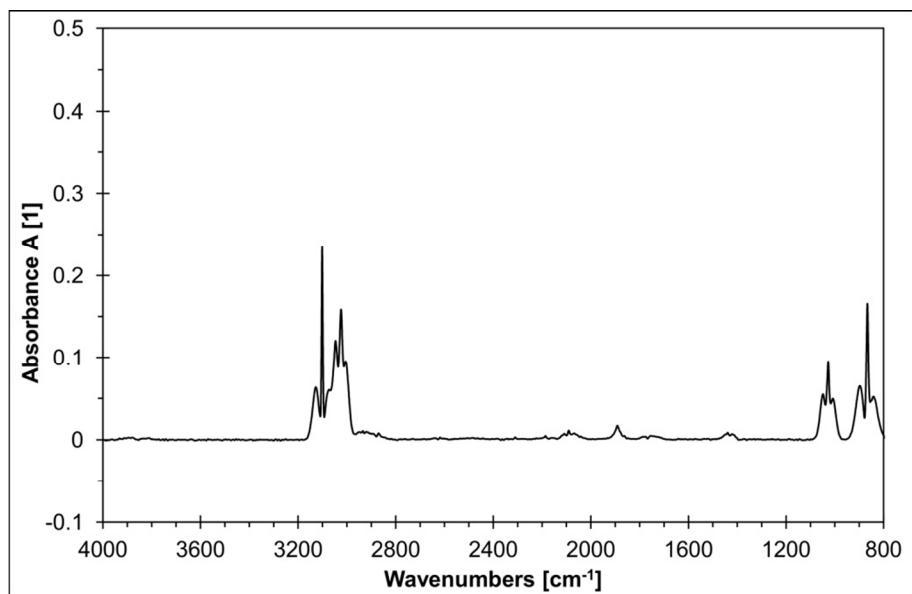


Figure S-7. Spectrum of cyclopropane; iHWG, 5000 ppm_v.

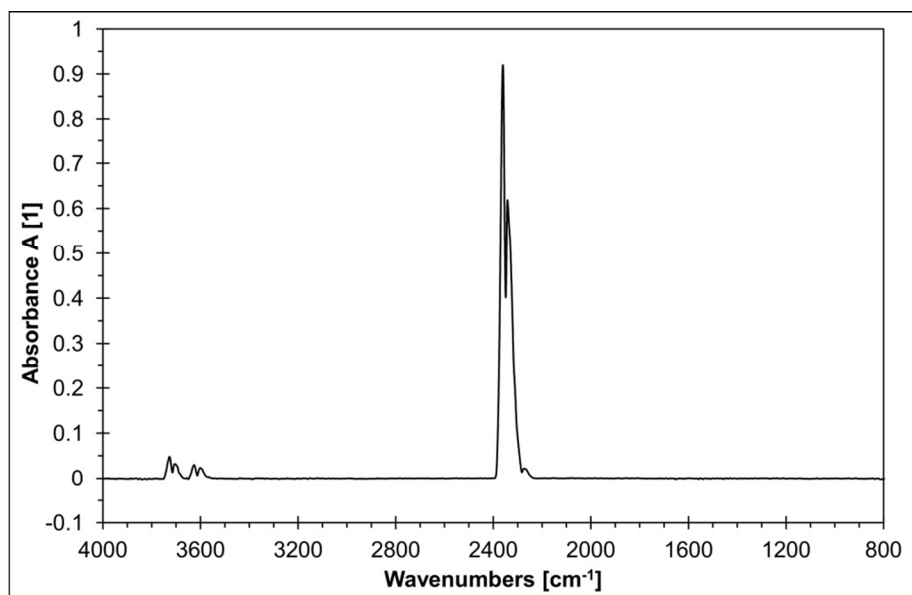


Figure S-8. Spectrum of carbon dioxide; iHWG, 5000 ppm_v.

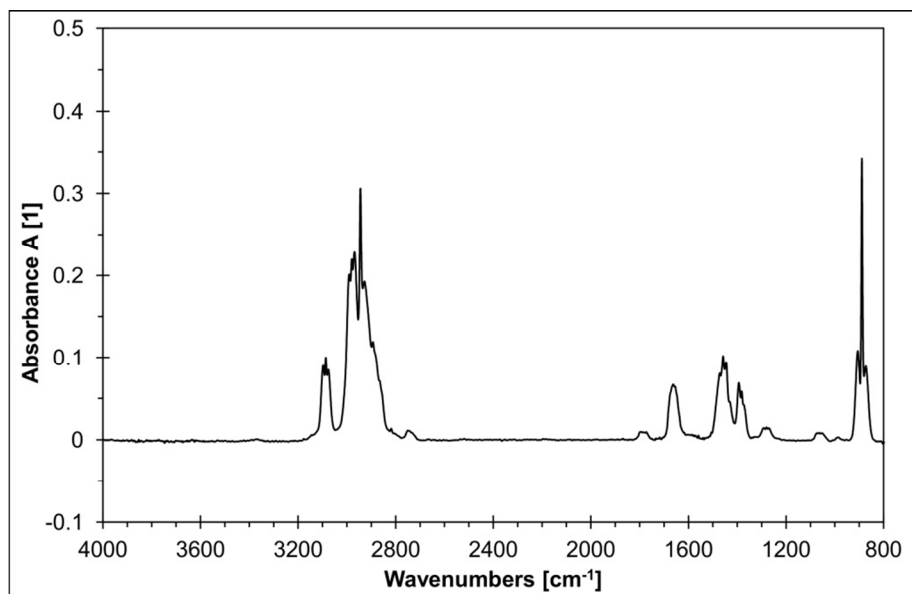


Figure S-9. Spectrum of isobutylene; iHWG, 5000 ppm_v.

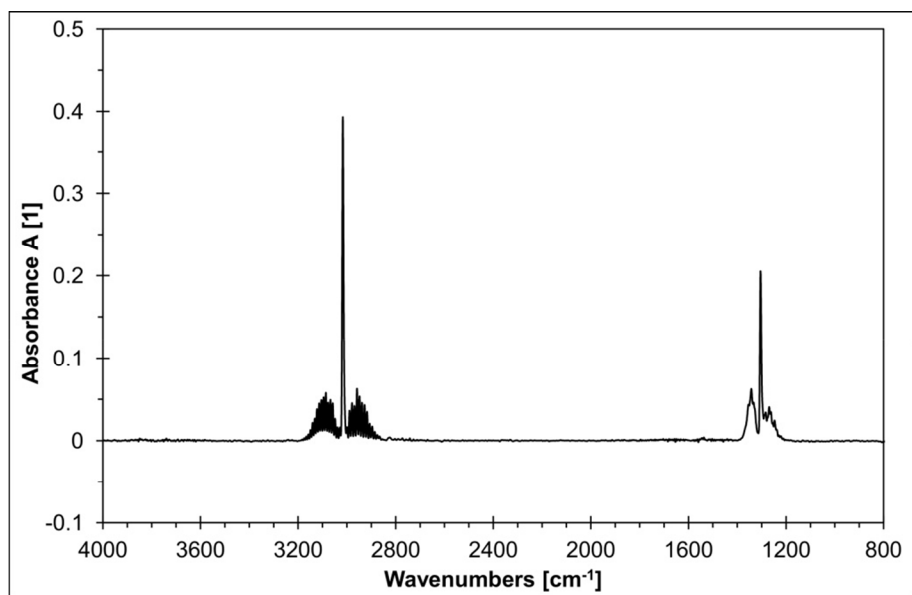


Figure S-10. Spectrum of methane; iHWG, 5000 ppm_v.

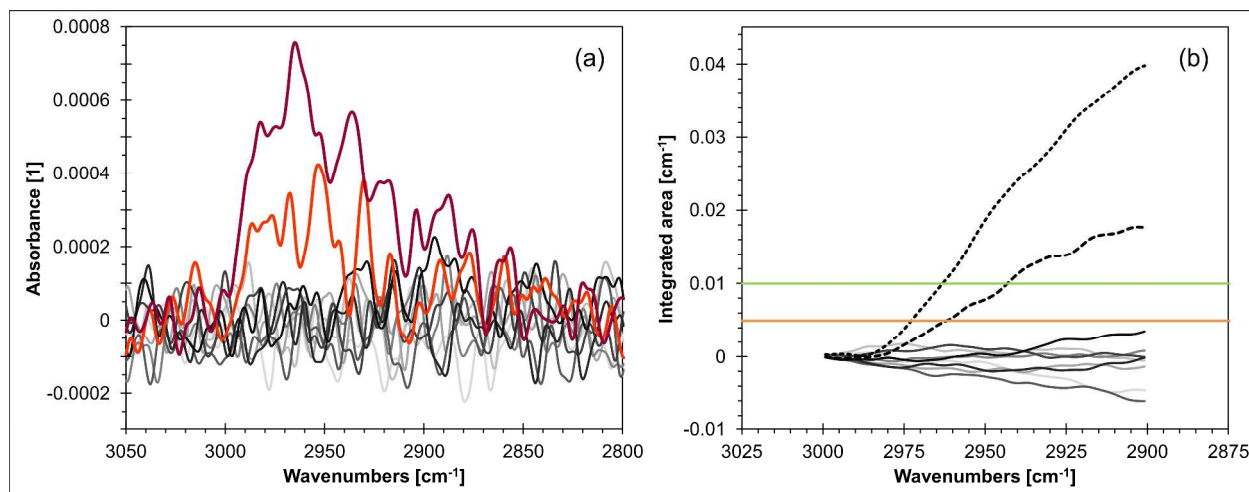


Figure S-11. Estimation of the LOD for butane. (a) Butane spectra of 3.3 ppm_v (red), and 6.7 ppm_v (purple) vs. 8 blank spectra (grey shades); 1000 averaged scans. (b) Integrated areas of all spectra (blanks = solid lines; 3.3 ppm_v butane = dashed line; 6.7 ppm_v butane = dotted line). The horizontal orange line denotes the decision criterion (compare Ref. 57) calculated as 1.65 times the standard deviation of the 8 blanks. The horizontal green line reflects the LOD. Both diagrams confirm that butane at 3.3 ppm_v may still be discriminated against a blank sample at these measurement conditions.